Folate-Conjugated Gold Nanoparticles

(Synthesis, Characterization and Design for Cancer Cells Nanotechnology-based Targeting)

A. R. Hashemian[1], H. Eshghi[2], G. A. Mansoori[3*], A. Shakeri-Zadeh[1,4] and A. R. Mehdizadeh[1,5]

1. Department of Medical Physics, Mashhad University of Medical Sciences, Mashhad, I. R. Iran
2. Department of Chemistry, Ferdowsi University of Mashhad, Mashhad, I. R. Iran
3. Departments of Bioengineering, Chemical Engineering & Physics, University of Illinois at Chicago, Chicago, USA
4. Department of Medical Physics, Iran University of Medical Sciences, Tehran, I. R. Iran
5. Department of Medical Physics, Shiraz University of Medical Sciences, Shiraz, I. R. Iran

(*) Corresponding author: mansoori@uic.edu

(Received: 15 Jul. 2009 and accepted: 25 Aug. 2009)

Abstract:

A new folate-conjugated gold nanoparticle (AuNP) has been designed to selectively target the folate receptor that is overexpressed on the surface of tumoral cells. For this purpose, we made 4-aminothiophenol, as a bifunctional linker to react with $HAuCl_4$ in the presence of sodium borohydride and it was binded to the AuNP surface through its thiol group. Then, we conjugated amino-terminated nanoparticles to folic acid with an amide-linkage formation.

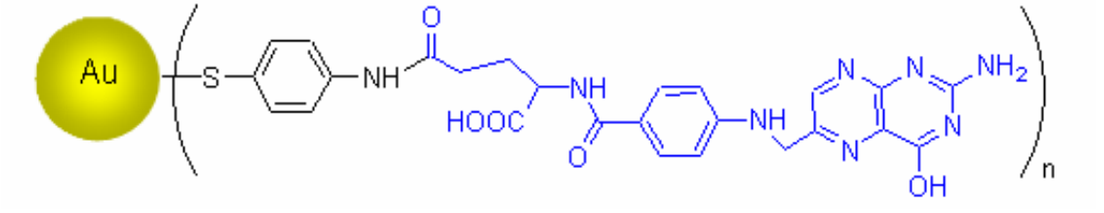

Finally, we evaluated the specific interaction between the folic acid and AuNP by the corresponding observed characteristic bands in the UV-vis and FTIR spectra. Transmission electron microscopic (TEM) images reveal the spherical AuNPs formation induced by the bifunctional linker. Powder X-ray diffraction (XRD) patterns confirmed the metallic face-centered cubic (FCC) lattice structure with (111), (200), (220), and (311) crystal planes. We estimated the average size of the conjugated nanoparticles to be about 5 nm by TEM and XRD. The Elemental analysis and atomic absorption showed 59 % organic molecules on the surface of AuNPs.

Keywords: *4-Aminothiophenol, AuNP, Cancer Cell Targeting, Conjugated Nanoparticle, Folate, Folate-conjugated gold nanoparticle, Folate Receptor, Folic Acid, Gold Nanoparticle, Nanotechnology.*

1. INTRODUCTION

There are many chemical compounds, of either natural origin or synthetic, which are effective as anticancer drugs. However, they cannot be used in conventional cancer therapy (chemotherapy) because of their toxicity to normal and healthy cells [1]. The limiting factor in the current cancer therapy is balancing acceptable damage resulted from these chemicals to, both, healthy and cancerous tissues. To overcome this problem and at the same time provide a broader range of therapeutic agents, such medicines may be delivered through a targeted system. Towards this goal, many researchers have been working on finding methods of increasing the efficacy of therapeutic agents by targeted therapy.

Nanotechnology-based targeting of cancer cells is one such promising approach to meet this goal. In this method, therapeutic agents attached to a nanoparticle, like gold nanoparticle, can specifically target a binding site on the surface of cancer cells [2]. Recently, a number of materials have been introduced and applied as targeting agents for therapeutic purposes. Folic acid is one such targeting agent [3]. Folic acid or folate (folic acid salt) is an important vitamin required for the healthy functioning of all cells. Folate is necessary for DNA nucleotide synthesis and cell division. A cancer cell will require much more folate than a healthy cell [4]. Folate is brought into, both, healthy and cancerous cells by the folate receptor. Folate receptor is used to transport folate into the cytosol of the cell for the synthesis of thymine by dihydrofolate reductase [5]. The presence of the folate receptor (FR) on a cell surface is regulated by the cell function. Cancer cells overexpress the FR because of their vast requirement for folate [6-8]. It has been proposed that because of the low expression level of FR in healthy cells and its overexpression in cancerous tissues, folate behaves as a suitable targeting agent [9-13]. Therefore, cancer cells display more FRs on their cell membrane. Accordingly, one should be able to target cancer cells by taking advantage of a cancer cell's appetite for folate.

On the other hands, nanotechnology [14] offers the opportunity to produce metallic nanoparticles holding many capabilities in cancer therapy. The synthesis of metallic nanoparticles has been the focus of extensive research over the past decade due to their particular properties [15,16]. Among these metallic nanoparticles, gold nanoparticle (AuNP) is of great interest for developing a unique system with high potential for biological applications such as nanophotothermolysis [17,18]. When short laser pulses irradiate AuNPs, a process named nanophotothermolysis occurs. In this process, AuNPs heat up quickly. It has been determined that the absorbed light by AuNP converts to heat on the picosecond time scale [19]. AuNPs are the most promising candidates for nanophotothermolysis since they are strong absorbers, photostable, nontoxic, and have adjustable optical properties [20]. The absorption maximum of AuNP is tunable from the mid visible region into the infrared region based on the size, shape and material [21]. AuNPs strongly absorb laser irradiation. This absorbed energy transforms quickly into heat, which could cause fatal damage to cancer cells through local overheating effects. Accordingly, AuNPs are potentially very practical and efficient photothermal agents in therapeutic applications, especially in cancer treatment [22,23].

With respect to the capabilities of AuNPs and through active targeting by folate, nanotechnology holds tremendous potential for the delivery of precisely targeted AuNPs that will reduce the collateral cell and tissue damage. The conjugation of AuNP with folic acid as a new system for the targeting of cancer cells is the main purpose of the present work. AuNPs cannot conjugate to folic acid directly and it is necessary to use a suitable linker, which has the capability to conjugate with them from two separate ends, simultaneously. To achieve this goal, we selected 4-aminothiophenol (4ATP) as a linker between AuNP and folic acid (Scheme 1).

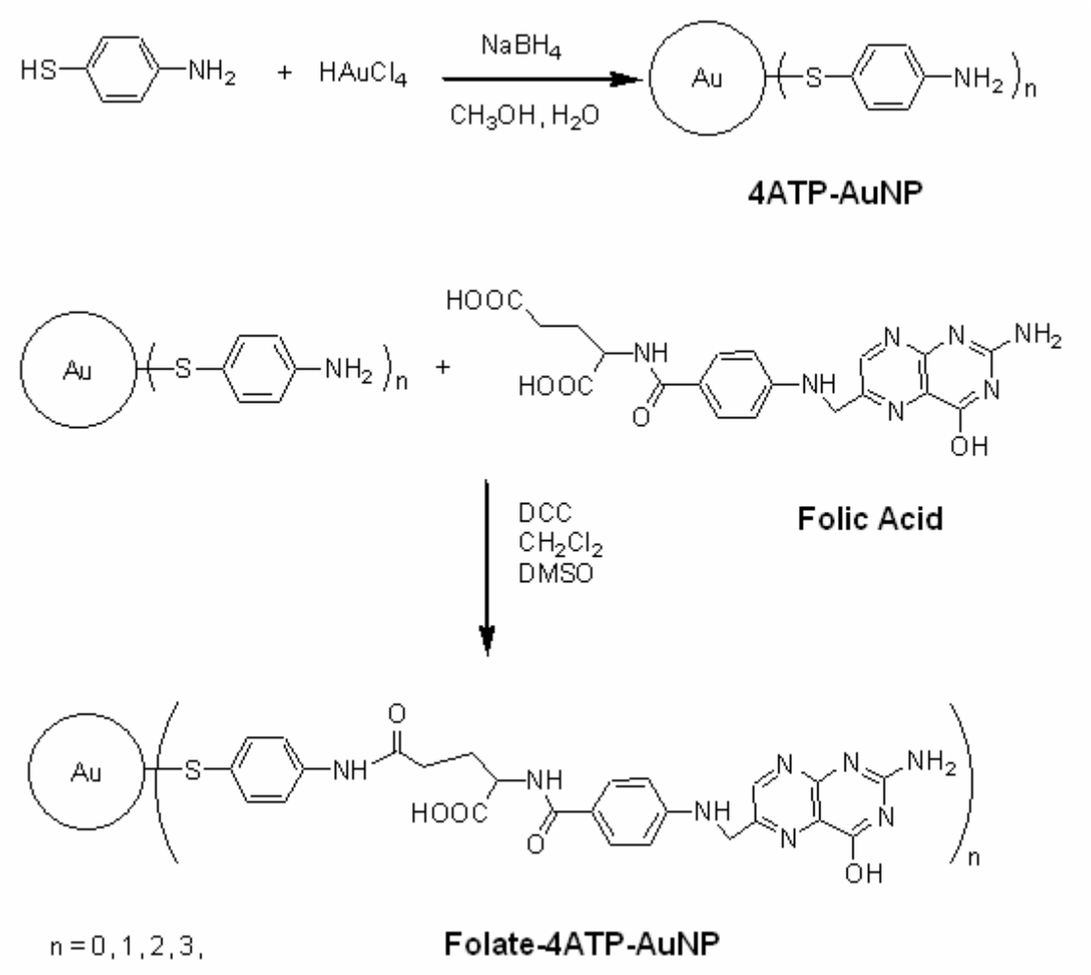

Scheme 1

In what follows we first present the experimental methods used to conjugate AuNP with folic acid. Then we discuss about our synthesis procedure and introduce our results. The results of various experiments which are performed to characterize and verify the properties of the conjugate produced are also reported.

2. EXPERIMENTAL METHODS

2.1. Materials

All the chemical compounds are used in this research were acquired from Merck, Germany and Fluka, Switzerland. Hydrogen tetrachloroaurate (III) trihydrate ($HAuCl_4.3H_2O$, 99.5% purity), 4-aminothiophenol (C_6H_7NS, 95% purity), Sodium borohydride ($NaBH_4$, 99.99% purity), and N, N'-dicyclohexylcarbodiimide ($C_{13}H_{22}N_2$, 99% purity) were purchased from Merck. Folic acid ($C_{19}H_{19}N_7O_6$, 97% purity) was obtained by Fluka, Switzerland.

2.2. Preparation of Gold Nanoparticles Conjugated with 4-Aminothiophenol (4ATP-AuNP)

A solution of $HAuCl_4.3H_2O$ (40 mg, 0.1 mM) in CH_3OH (10 mL) was added to a stirred solution

of 4- aminothiophenol (4ATP, 75 mg, 0.6 mM) in CH_3OH (10 mL). After 20 minutes of stirring, a freshly prepared solution of sodium borohydride (57 mg, 1.5 mM) in deionized water (5 mL) was added to the vigorously stirred reaction mixture drop-wise in a 15 min period. The reaction mixture turned deep brown indicating the formation of AuNPs. The stirring was continued for one hour. Finally, the conjugation of AuNP and ATP were separated from methanol by precipitation under centrifuge at 10,000 rpm and purified by successive washing with CH_2Cl_2 and deionized water. Ultrasound sonication was performed to disperse the nanoparticles into the base material thoroughly. Subsequently, centrifuging and washing with deionizer water was carried out to reach additional purification. We obtained the conjugation of 4ATP-AuNP after drying and the results were stored for further characterization and reactions.

2.3. Preparation of Folate-Conjugated Gold Nanoparticle (Folate-4ATP-AuNP)

A solution of folic acid (22 mg, 0.05 mM) in DMSO (5 mL) was added to a pre-sonicated colloids of 4ATP-AuNP (8 mg) in CH_2Cl_2 (10 mL). The orange mixture that resulted was vigorously stirred for 20 min. After this time, a solution of N, N'-dicyclohexylcarbodiimide (DCC) (11 mg, 0.05 mM) in CH_2Cl_2 (10 mL) was added to the orange mixture drop-by-drop while stirring. The stirring was continued for ten hours and a green-color mixture was obtained. The final product was separated by fast centrifugation. It was subsequently washed with CH_2Cl_2. To obtain more purification, ultrasound sonication was carried out and then the mixture was centrifuged and washed with deionized water again. The final product (Folate-4ATP-AuNP) was obtained as a powder after drying. This powder exhibited a golden color in reflection.

2.4. Characterization Techniques

UV-visible (UV-vis) absorption spectroscopic measurements were recorded on a single beam UV-vis spectrometer, Agilent 8453, using quartz cells of 1 cm path length and methanol as the reference solvent at room temperature. Also, Fourier Transform Infra Red (FTIR) measurements were recorded on a Shimadzu FT-IR 4300 instrument using KBr pellets at room temperature. Transmission electron microscopic (TEM) images of the nanoparticles were taken with a LEO 912AB instrument operated at an accelerating voltage of 120 kV with line resolution of 0.3 nm at room temperature. The samples for TEM measurements were prepared by placing a droplet of the colloidal solution onto a carbon-coated copper grid and allowing it to dry in air naturally. X-ray diffraction (XRD) was carried out with a Bruker D8 ADVANCE X-ray Diffractometer, using the wavelength of 0.15406 nm (Cu Kα) radiations at room temperature. Based on the TEM images we determined the size distributions of the final product by counting at least 300 particles. The elemental analyses for carbon, hydrogen, nitrogen, sulfur and oxygen were performed using a Thermo-Finnigan CHNS-O analyzer. We determined the gold percentage in the Folate-4ATP-AuNP by Shimadzu model AA-670 atomic absorption spectrophotometer.

3. RESULTS

We synthesized AuNPs according to the standard wet chemical methods [24] using sodium borohydride as a reducing agent. Folate-conjugated AuNPs were prepared using 4ATP as the linker as shown in Scheme 1. 4ATP reacts with HAuCl4 in aqueous methanol solution at room temperature to form dark brown 4ATP-stabilized gold nanoparticles (4ATP-AuNP). In this conjugation, 4ATP as a bidentate spacer attaches to the AuNP via its sulfur atom. 4ATP has been selected for binding to AuNP because it is –SH terminated and its oxidation in the attachment to AuNP is well known [24,25]. There is also, NH_2 group at the other side of 4ATP molecule, which is suitable for conjugation to folate. Our preference for the choice of amide bond formation in the attachment of folate to AuNP is its stronger bond as compared to other linkers such as thioesters [26]. Ester and thioester hydrolysis may be problematic in the physiologic transfer of drug to the target cells.

Because of the bonding procedure mentioned above we obtained the folate conjugated gold nanoparticles (Folate-4ATP-AuNP for short) which is a clean colloid with green color. It was then separated and precipitated through centrifugation. We clearly identified the formation of such conjugations from their UV-visible and FTIR spectra.

Figure 1 shows the FTIR spectrum of 4ATP-AuNP as compared with the spectrum of neat 4ATP. According to this Figure, the infrared spectrum of 4ATP-AuNP shows the characteristic bands of NH_2 group in 3440 and 3325 cm^{-1} wavelengths. With regard to the spectrum of 4ATP-AuNP in comparison to the spectrum of 4ATP, it can be found that the SH stretching vibration (2560 cm^{-1}) has disappeared. As a result, the formation of S-Au bond can be inferred because significant changes in many characteristics of thiol vibrations have been occurred. In addition, the intensity of some of the vibrations in the fingerprint region has been decreased or disappeared. These all confirm that the bonding of 4ATP to the AuNP surface has been taken place through the SH group.

AuNPs possess the characteristic surface plasmon absorption at 520 nm in the UV-visible absorption spectrum [24]. This characteristic absorption band in the assemblies of AuNPs interlinked by various molecules exhibit a peak between 520 and 620 nm [27]. Because of the propensity for intermolecular hydrogen bonding in the assemblies of AuNPs interlinked by different ligands, resultant broadening and red-shifting of the plasmon absorption peak are to be expected. It is worthy to note that this is the most prominent in the case of assemblies of AuNPs interlinked by 4ATP [24,27]. Also, λmax of these assemblies (AuNPs-Ligands) is dependent on the particle size [28]. Accordingly, a significant broadening of the gold surface plasmon bands or the appearance of a red-shifted absorption band due to coupling of the individual surface plasmon of nanoparticles in the aggregated structures will be observed if the interlinked nanostructures are formed.

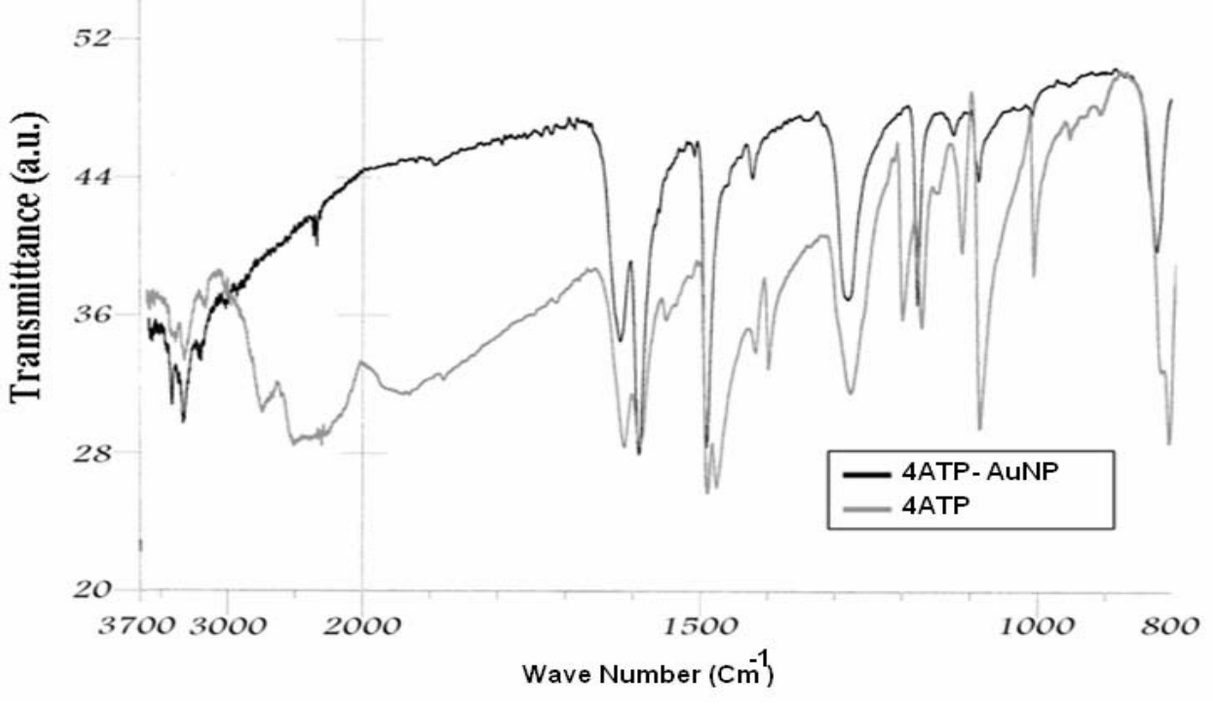

Figure 1: FTIR spectra versus wave number of 4ATP-AuNP in comparison to 4ATP.

Figure 2 shows the UV-vis spectra of the synthesized 4ATP-AuNP and Folate-4ATP-AuNP conjugated gold nanoparticles. In the spectrum of 4ATP-AuNP, the appearance of surface plasmon bands around 560 nm confirms the formation of stable gold nanoparticles. Moreover, according to the literature [29], the absorption maxima at 280 and 360 nm can be used for confirming the covalent attachment of the folate with ATP-AuNP. By studying the UV-Visible absorption spectrum, we determined that Folate-4ATP-AuNP has the absorption peaks at 275 nm and 362 nm pertaining to folate and absorption peak at 564 nm pertaining to AuNP.

Figure 3 shows the FTIR spectra of Folate-4ATP-AuNP in comparison to 4ATP-AuNP. According to this Figure, the FTIR spectrum of Folate-4ATP-AuNPs shows the strong carbonyl absorbance at 1700 cm^{-1} due to –CONH- and α-COOH groups stretching of folate conjugate. In addition, the bands at 3500, 3375, and 3200 cm^{-1} correspond to the NH_2 and amide NH stretches of folate conjugate, respectively. Additionally, the bands at 835, 1190, and 1290 cm^{-1} correspond to the out-of plane and in plane motions of NH_2, and C-N stretch of folic acid (not showed) and ATP-AuNP conjugate are shifted to 855, 1220, and 1320 cm^{-1}, respectively. These all indicate the formation of folate conjugation in the Folate-4ATP-AuNP.

Elemental analysis of Folate-4ATP-AuNPs determined by Carbon Hydrogen Nitrogen Sulfur Oxygen (CHNS-O) Analysis and Atomic Absorption Spectrometry resulted in {C=28.7%; H=2.5%; N=13.3%; S=3.5%; and Au=41.3%; O=10.7%}. The C:H=11.48 and S:H=1.4 ratios are, within the experimental uncertainties, equal to those of the Folate-4ATP conjugate.

We report the transmission electron microscopic (TEM) image of the synthesized Folate-4ATP-AuNP and the relevant size histogram in Figure 4. The size histograms (Figure 4, inset) of the Folate-4ATP-AuNP nanoparticles are determined by counting at least 300 particles. The nanoparticles' shape is nearly spherical and the micrographs clearly indicate the formation of nearly monodispersed

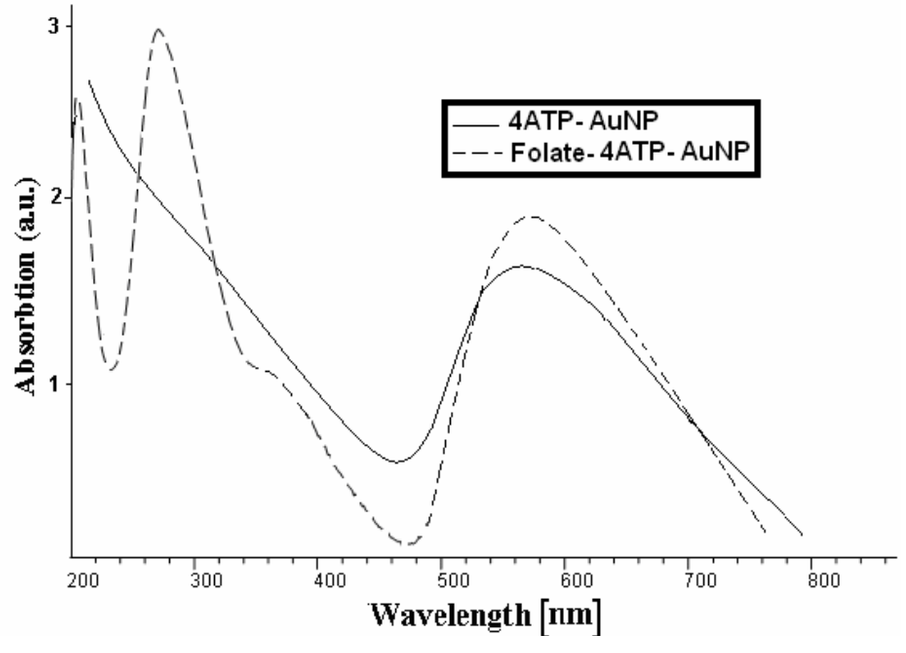

Figure 2: UV-Visible absorption spectra versus wavelength of 4ATP-AuNP and Folate-4ATP-AuNP.

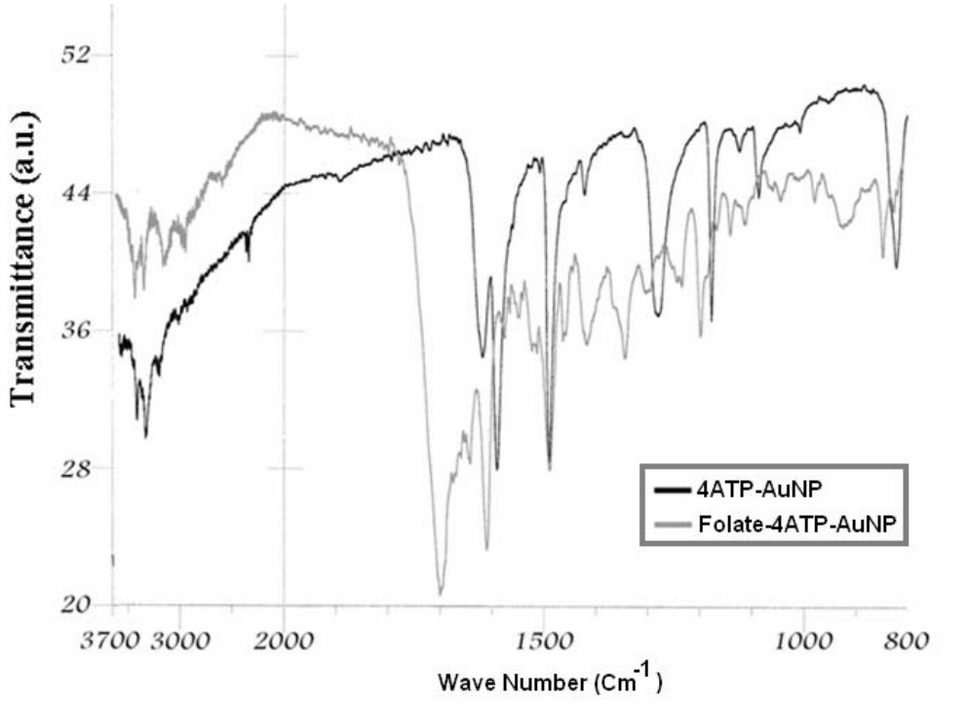

Figure 3: FTIR spectra of Folate-4ATP-AuNP versus wave number in comparison to 4ATP-AuNP.

nanoparticles with an average diameter of 5 nm. As shown in Figure 5, the crystalline nature of these nanoparticles is confirmed through the X-ray diffraction (XRD) analysis, where (111), (200), (220), and (311) crystal planes of metallic face-centered cubic (FCC) structure are identified with a lattice constant of 0.407376 nm.

4. CONCLUSION

The synthesis and characteristics of a new folate-conjugated gold nanoparticles using 4-aminothiophenol (4ATP) as a linker were reported. UV-visible and FTIR spectroscopy confirms the attachment of folic acid to the gold nanoparticles. We confirm the crystalline nature of the final product by TEM micrographs and XRD spectroscopy. Using the data obtained from elemental analysis techniques such as CHNS-O Analysis and Au Atomic Absorption Spectrometry, the conjugation of organic chains (Folate-4ATP) with AuNPs are confirmed.

Because this new and original synthesized complex material contains folate, it can be applied to selective targeting of folate receptor positive cancerous cells, which overexpress folate receptor on their surface. Significant absorption of this new synthesized complex makes it a promising material for using in the area of cancer therapy and thermal ablation of tumors. Further investigations in cellular targeting by these new folate-conjugated gold nanoparticles are in progress in our laboratories.

Acknowledgments: The conceptual design of this report was originally suggested by M. Kent, K.S. Brandenburg and D. Swan, as a bioengineering senior design project under supervision of Dr. G.A. Mansoori and received one of the highest awards during the 2006 UIC Engineering Expo. This research is supported, in part, by the MUMS Council for Research under Grant # 85310. We would like to thank Professor S. F. Tayyari for his helpful contribution in doing FTIR spectroscopy.

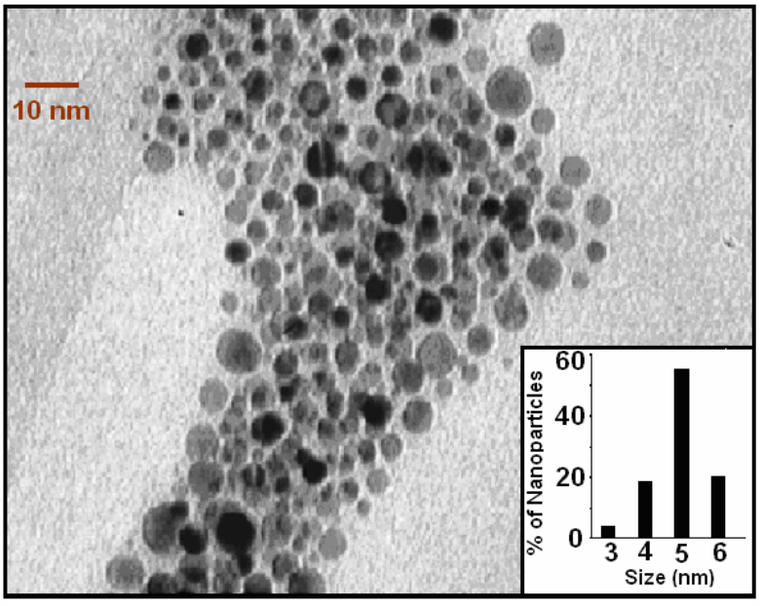

Figure 4: TEM photograph of Au nanoparticles in Folate-4Atp-AuNP nanocongugate and histogram for the size distribution of Au nanoparticles.

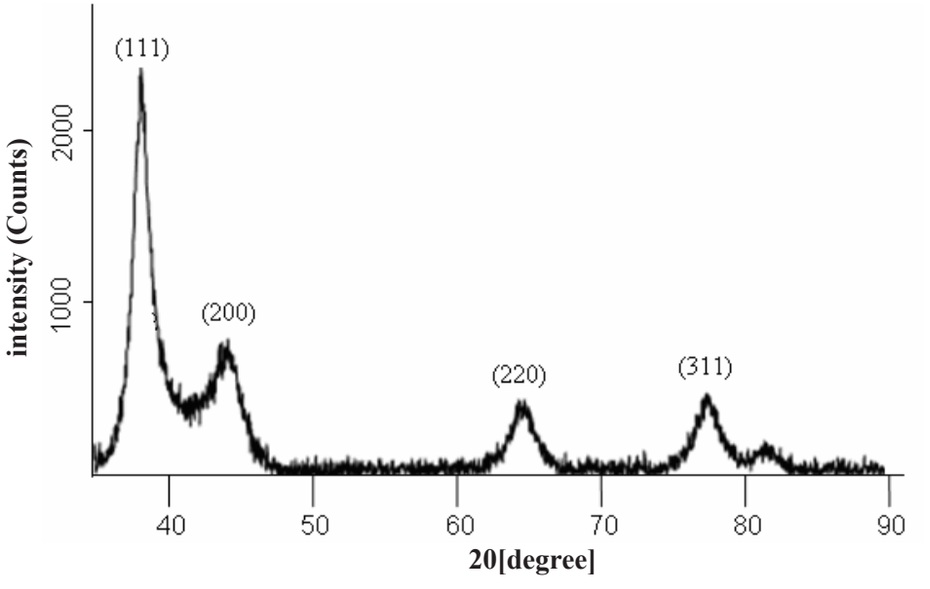

Figure 5: XRD pattern of Au nanoparticles in Folate-4ATP-AuNP.

Abbreviations	
AuNP	Gold nanoparticle
DMSO	Dimethylsulfoxide
4Atp	4- aminothiophenol
Folate-4Atp-AuNP	Folate-Conjugated Gold Nanoparticle through 4- aminothiophenol
DCC	N,N'-dicyclohexylcarbodiimide
FTIR	Fourier Transform Infra Red
TEM	Transmission electron microscopic
XRD	X-ray diffraction
FCC	Face centered cubic

References

1. Neil, M. S. J. Leukocyte. Biol. 2005, 78, 585-594.
2. Sinha, R.; Kim, G. J.; Nie, S.; Shin, D. M. Mol. Cancer Therapy. 2006, 5, 1909-1917.
3. Yoo, H. S.; Park, T. G. J. Control Release. 2004, 100, 247–256.
4. Doucette, M. M.; Stevens, V. L. J. Nutrition. 2001, 131, 2819-2825.
5. Antony, A. C. Blood 1992, 79, 2807-2820.
6. Toffoli, G.; Cernigoi, C.; Russo, A.; Gallo, A.; Bagnoli, M.; Boiocchi, M. Int. J. Cancer 1997, 74, 193–198.
7. Hasegawa, T.; Fujisawa, T.; Haraguchi, S.; Numata, M.; Karinaga, R.; Kimura, T.; Okumura, S.; Sakurai K.; Shinkai, S. Bioorg. Med. Chem. Lett. 2005, 15, 327-330.
8. Henne, W. A.; Doorneweerd, D. D.; Hilgenbrink, A. R.; Kularatne, S. A.; Low, P. S. Bioorg. Med. Chem. Lett. 2006, 16, 5350-5355.
9. Stella, B.; Arpicco, S.; Peracchia, M. T.; Desmaele, D.; Hoebeke, J.; Renoir, M.; D'Angelo, J.; Cattel, L.; Couvreur, P. J. Pharmaceutical. Sci. 2000, 89, 1452–1464.
10. Leamon, C. P.; Reddy, J. A. Adv. Drug Delivery Review. 2004, 56, 1127– 1141.
11. 11. Wiener, E. C.; Konda, S.; Shadron, A.; Brechbiel, M.; Gansow, O. Investigative Radiology. 1997, 32, 748-754.
12. Yoo, H. S.; Park, T. G. J. Control Release 2004, 100, 247–256.
13. Gabizon, A. T.; Horowitz, D.; Goren, D.; Tzemach, D.; Mandelbaum-Shavit, F.; Qazen, M. M., Zalipsky, S. Bioconjug. Chem. 1999, 10, 289–298.
14. Mansoori, G. A. Principles of Nanotechnology-Molecular-Based Study of Condensed Matter in Small Systems, World Scientific Pub. Co., Hackensack, NJ, USA, 2005.
15. Mansoori, G. A.; George, T. F.; Assoufid, L.; Zhang, G. (Eds.), Molecular Building Blocks for Nanotechnology: From Diamondoids to Nanoscale Materials and Applications, Springer, New York, Topics in Applied Physics Vol 109, 2007.
16. Sharma, J.; Mahima, S.; Kakade, B. A.; Pasricha, R.; Mandale, A. B.; Vijayamohanan, K. J. Phys. Chem. B. 2004, 108, 13280-13286.
17. Daniel, M. C.; Astruc, D. Chemical Reviews. 2004, 104, 293-246.
18. Basak, A.; Bag, S. S.; Basak, A. Bioorganic and Medicinal Chemisty. 2005, 13, 4096-4102.

19. Link, S.; El-Sayed, M. A. International Reviews in Physical Chemistry. 2000, 19, 409–453.

20. Zharov, V. P.; Mercer, K. E.; Galitovskaya, E. N.; Smeltzer, M. S. Biophys. J. 2006, 90, 619-627.

21. El-Sayed, I. H.; Huang, X.; El-Sayed, M. A. Nano Letter. 2005, 5, 829 -834.

22. El-Sayed, I. H.; Huang, X.; El-Sayed, M. A. Cancer Letter. 2006, 239, 129–135.

23. Mansoori, G. A.; Mohazzabi, P.; McCormack, P.; Jabbari, S. Nanotechnology in cancer prevention, detection and treatment, World Review of Science, Technology and Sustainable Development, 4(2/3):226-257, 2007.

24. Shi, W.; Sahoo, Y.; Swiharta, M. Colloids Surf. A Physicochem. Eng. Asp. 2004, 246, 109–113.

25. Johnson, S. R.; Evans S. D.; Brydson R. Langmuir. 1998, 14, 6639-6647.

26. (a) Smith, M. B.; March, J. March's Advanced Organic Chemistry: Reactions, Mechanisms, and Structure, Sixth Edition, John Wiley & Sons, New York, USA, 2007; (b) Carey, F. A.; Sundberg, R. J. Advanced Organic Chemistry, Part A, Fifth Edition, Springer, New York, USA, 2007.

27. Wessels, J. M.; Nothofer, H. G.; Ford, W. E.; Wrochem, F. V.; Scholz, F.; Vossmeyer, T.; Schroedter, A.; Weller, H.; Yasuda, A. J. Am. Chem. Soc. 2004, 126, 3349-3356.

28. Link, S.; El-Sayed, M. A. J. Phys. Chem. B. 1999, 103, 4212-4217.

29. Pan, D.; Turner, J. L.; Wooley, K. L. Chem. Commun. 2003, 19, 2400–2401.

30. Zhang, Z.; Zhou, F.; Lavernia. E. J. Metall. Mater. Trans. A, 2003, 34, 1349-1355.